Available online at www.sciencedirect.com
SCIENCE DIRECT®
Agricultural and Forest Meteorology 117 (2003) 1–22
AGRICULTURAL AND FOREST METEOROLOGY
www.elsevier.com/locate/agrformet

Transpiration in a small tropical forest patch

Thomas W. Giambelluca [a,*], Alan D. Ziegler [a], Michael A. Nullet [a], Dao Minh Truong [b], Liem T. Tran [c]

[a] *Department of Geography, University of Hawaii at Manoa, 2424 Maile Way, Honolulu, HI 96822, USA*
[b] *Center for Natural Resources and Environmental Studies, Vietnam National University, Hanoi, Viet Nam*
[c] *Earth System Science, Pennsylvania State University, University Park, PA 16802, USA*

Received 12 July 2002; received in revised form 3 February 2003; accepted 6 February 2003

Abstract

A field study was conducted of microclimate and transpiration within a 12 ha patch of advanced secondary forest surrounded by active or recently abandoned swidden fields. Differences in microclimate among stations located within and near the patch, give evidence of the effects of the adjacent clearing on the environment in the patch.

Volumetric soil moisture content at the end of the dry season was lowest at the two edge sites, suggesting greater cumulative dry season evapotranspiration (ET) there than at swidden and forest interior sites. Total evaporation, based on energy balance methods, was also higher at the two edge sites than at the swidden or forest interior sites. Spatial differences in evaporation decreased as conditions became wetter.

Measurements of sap flow in nine trees near the southwestern edge of the patch and nine trees in the patch interior indicate considerable variability in transpiration among the three monitored tree species, *Vernicia montana*, *Alphonsea tonkinensis*, and *Garcinia planchonii*. Dry-period transpiration averaged about 39 and 43% of total evaporation for edge and interior trees, respectively, increasing to 60 and 68% after the start of rains. Transpiration in both zones was well-correlated with micrometeorological conditions in the adjacent clearing, implying that transpiration edge effect is greatest when conditions are favorable for high positive heat advection from the clearing to the forest edge. Transpiration rates of well-exposed trees were higher than poorly-exposed trees, and decreased with distance from the edge at a statistically significant rate of −0.0135 mm per day m^{-1}. Although the results on the strength of transpiration edge effect are somewhat equivocal due to variability within the small sample, there is clear evidence that ET within the patch is influenced by the surrounding clearings. If edges experience higher ET, greater fragmentation would result in higher regional evaporative flux, which would partly compensate for the reduction in regional ET due to deforestation.

Keywords: Forest fragmentation; Forest hydrology; Tropical deforestation; Sap flow; Edge effect; Microclimate; Evapotranspiration

1. Introduction

The global rate of tropical deforestation exceeds 150,000 km^2 per year (Whitmore, 1997). This alarmingly rapid land cover conversion raises concerns regarding reduction of plant and animal biodiversity, impacts on the cultures of indigenous peoples, modification of atmospheric chemistry and consequent global climate impacts, and regional to global climatic and hydrologic effects of changing land surface–atmosphere interaction. The remaining forest in much of the tropics is confined to increasingly

* Corresponding author. Tel.: +1-808-956-7683; fax: +1-808-956-3512.
E-mail address: thomas@hawaii.edu (T.W. Giambelluca).

0168-1923/03/$ – see front matter © 2003 Elsevier Science B.V. All rights reserved.
doi:10.1016/S0168-1923(03)00041-8

small patches of remnant primary and secondary forest. As Laurance and Bierregaard (1997) observe, "fragmented landscape is becoming one of the most ubiquitous features of the tropical world—and indeed, of the entire planet." Especially in the tropics, small forest fragments are decreasing in size as forest edges recede due to the effects of human disturbance in the surrounding matrix (Gascon et al., 2000) Increasing fragmentation of tropical land cover is generally perceived to have negative ecological impacts, including alteration of the near-edge microclimate (Laurance et al., 1998). Effects of fragmentation on regional climate and hydrology are less well known.

Forest clearing is known to disrupt land surface–atmosphere exchange of energy and mass by altering the physical characteristics of the land surface. In general, deforestation increases surface albedo and reduces net radiation (e.g. Giambelluca et al., 1997, 1999). Forest removal affects evaporation[1] by changing surface albedo, leaf area, aerodynamic roughness, root depth, and stomatal behavior. Field studies have confirmed that evaporation is significantly reduced when tropical forest is replaced by pasture (e.g. Jipp et al., 1998; Wright et al., 1992). As a result of decreased evaporation, stream discharge increases following deforestation (Bruijnzeel, 1990, 2001). The effects of land cover change may also lead to regional changes in atmospheric circulation and rainfall. For example, general circulation model (GCM) simulations of the complete conversion of the Amazon rainforest to grassland, predict large reductions in basin precipitation (Henderson-Sellers and Gornitz, 1984; Lean and Warrilow, 1989; Shukla et al., 1990; Nobre et al., 1991; Henderson-Sellers et al., 1993; Polcher and Laval, 1994; McGuffie et al., 1995; Xue et al., 1996; Hahmann and Dickinson, 1997). The rainfall decrease is attributed, in part, to lower evaporation in the basin, and consequent reduction in 'recycling' of evaporated water into additional basin rainfall (Henderson-Sellers et al., 1993).

Estimating evaporation for regions with heterogeneous land cover is an important part of the problem of scaling energy, water, and momentum fluxes (Veen et al., 1991), which has been undergoing intensive research (Kienitz et al., 1991; Stewart et al., 1996; Famiglietti and Wood, 1994, 1995). A simple mosaic approach can be used to take account of the relative proportions of the dominant land cover types by computing area-weighted averages of the fluxes over each land cover type (e.g. Liang et al., 1994). However, patch-scale fluxes are not independent of the surroundings. Horizontal transfer of energy and water vapor in the atmosphere may significantly alter the fluxes within a patch and hence invalidate a strictly one-dimensional approach to estimating regional average fluxes. Such effects are greatest at the boundaries of dissimilar land covers (Veen et al., 1991, 1996; Kruijt et al., 1991; Klaassen, 1992; Klaassen et al., 1996). Near the upwind margin of a forest patch, processes are influenced by the advection of sensible energy generated in the clearing and by turbulence generated at land cover boundaries. Air entering a forest edge is relatively warm, dry, and turbulent, thus increasing evaporation potential. This edge effect diminishes with distance toward the patch interior, but remains significant for several tens of meters. As Veen et al. (1991) noted, "regional evaporation may be higher in a landscape with many patches of forest (many edges) as compared with a landscape with the same total forest concentrated in large blocks." This dependency of regional latent energy flux on the scale of landscape fragmentation was also shown by Klaassen (1992) using a surface layer model.

Measurements of transpiration near forest edges are sparse, due in part to the difficulties posed in field measurements near surface discontinuities (cf. Gash, 1986). The few field observations which have been made generally give evidence supporting the depiction of the forest edge as a "special high-flux environment" (Veen et al., 1996). For example, at a site 200 m downwind of a forest edge, Hutjes (1996) (cited in Veen et al., 1996) observed turbulent energy fluxes to the atmosphere (sum of latent and sensible energy fluxes) up to 25% greater than net radiation. Theory suggests that evaporation of intercepted rainfall would be especially influenced by edge effect. In fact, simulations by Veen et al. (1991) suggested that edge effects would be maximal for a wet canopy, while dry canopy transpiration would be affected very little. Contrary to those expectations, throughfall measurements (e.g. Neal et al., 1993) show almost no relationship with distance from the forest edge. Klaassen et al. (1996) concludes that proximity to the edge affects both the

[1] In this paper, except when otherwise specified, "evaporation" and "evapotranspiration" are equivalent.

interception storage capacity and the rate of evaporation of intercepted water, which cancel one another. However, he speculates that the forest edge dries more quickly, allowing transpiration to begin sooner after a storm.

Other researchers have found indirect evidence of greater evaporative flux near the forest edge. Working in isolated forest reserves in central Amazonia, Kapos (1989) found lower soil moisture within 10–20 m of the forest margins. Studies of forest patch microclimate generally show significant gradients in temperature, humidity, solar radiation, and wind speed at levels within and beneath the canopy (Matlack, 1993; Chen et al., 1993; Murcia, 1995; Kapos et al., 1997; Turton and Freiburger, 1997), which may suggest trends in evaporation. Detectable effects generally were found to extend as far as 20–50 m into the forest, with the extent sometimes dependent on edge aspect, edge age, or patch size.

Most studies of edge microclimate and turbulent fluxes have been conducted over flat terrain. This is done to minimize the effects arising from heterogeneities other than those associated with land cover. Steep terrain further hampers the use of micrometeorological approaches to flux measurement and complicates the interpretation of results. However, in parts of the tropics where landscape fragmentation is most pronounced, such as montane Southeast Asia, studies on flat terrain are impossible and perhaps irrelevant.

Theory strongly suggests that forest edges downwind of land with lower vegetation or bare soil will experience higher rates of evaporation due to positive energy advection and enhanced turbulence. So far, empirical evidence of this process is limited and sometimes contradictory. Efforts are intensifying to understand the effects of spatial heterogeneity and incorporate them into land surface–atmosphere schemes and regional hydrologic models. The need to understand and quantify edge effects on transpiration increases as the tropical landscape continues to become more fragmented. With this in mind, we conducted a field study of the spatial variations in microclimate and transpiration in a 12 ha forest patch in Ban Tat hamlet, Hoa Binh, Vietnam. The objectives of this study were to determine: (1) the effects of adjacent clearings on the microclimate of a small forest patch, (2) the extent to which transpiration by trees is dependent on distance from the edge of the patch, (3) whether transpiration edge effects vary by season (dry–wet); and (4) the effects of variations in atmospheric conditions on the spatial pattern of transpiration.

2. Field methodology

Our research strategy called for a measurement transect through a small forest patch oriented along the prevailing wind direction (Fig. 1). We selected a 12 ha patch of advanced secondary forest surrounded by active or recently abandoned swidden fields. A narrow strip of younger secondary vegetation bordered the northeastern side of the forest patch. We focused our observations on the southwest-facing forest edge (Fig. 2) because of its distinct boundary, the high contrast provided by its neighboring patch, and the expectation of frequent southwest winds (regional wind direction during most of our observations were dominantly southwest, however, terrain and local thermal influences produced mostly northwesterly or northeasterly surface winds at the site). Other forest edge sites considered during an extensive ground survey were rejected due to excessively steep slope.

To monitor microclimate variation within and near the patch, we installed stations at four sites along a

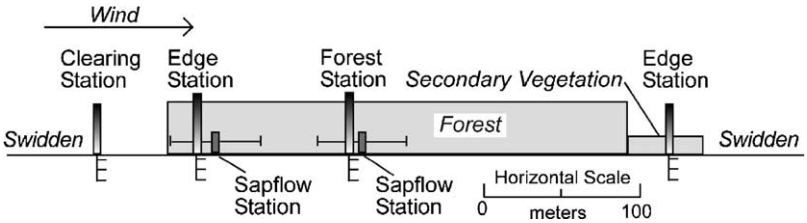

Fig. 1. Diagram showing idealized experimental design for investigation of forest patch microclimate and transpiration edge effect at Ban Tat Hamlet, northern Vietnam.

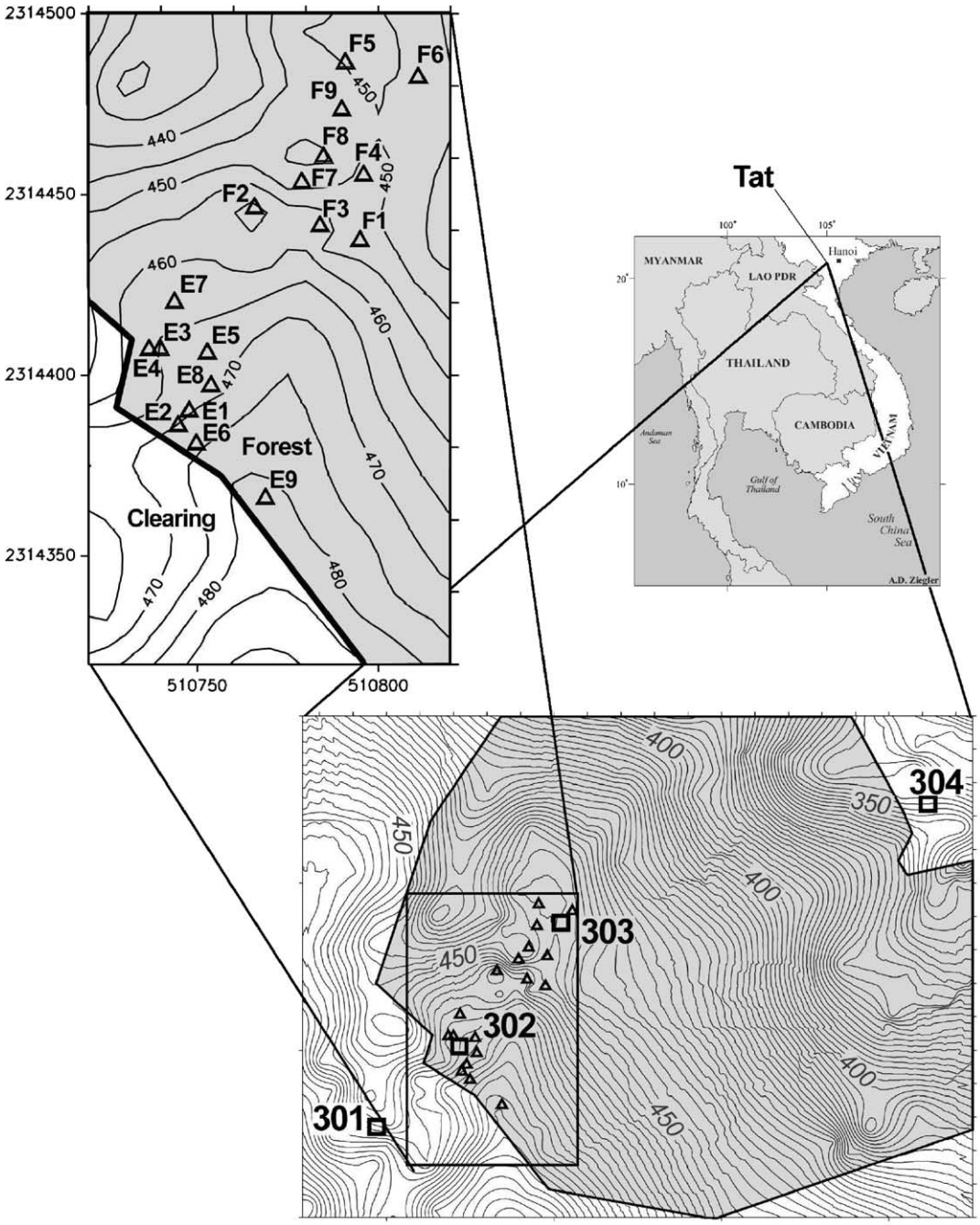

Fig. 2. Map of the study site showing the location of Tat Hamlet in northern Vietnam, the locations of the four meteorological stations (squares) and 18 trees (triangles) monitored for sap flow in relation to the forest patch boundary (forest is shaded) and elevation (m a.s.l.). In the upper left panel, UTM coordinates (m) are given for scale.

Table 1
Meteorological observations

Station site		Height (m)			
Sensor[a]	Type[b]	301 Swidden field	302 Forest edge	303 Forest interior	304 Secondary vegetation edge
R_{net}	REBS*7	2.7	–	13.57	–
K_d	Eppley 8-48	2.85	–	–	–
K_u	Eppley 8-48	2.85	–	13.5	–
T_{ir}	Everest 4000	2.7	12.1	13.5	4.57
T_a/RH	Met-One 083C	3.0	12.3	14.05	5.07
U/WD	Met-One 034A	3.25	12.55	14.25	5.42
RF	Met-One	0.75	–	–	–
G	REBS HFT-3	−0.08	–	−0.08	–
T_{soil}	CSI TCAV	−0.02, −0.06	–	−0.02, −0.06	–
SM_1	CSI CS615	0.0 to −0.3	0.0 to −0.3	0.0 to −0.3	0.0 to −0.3
SM_2	CSI CS615	−0.5 to −0.8	−0.5 to −0.8	−0.5 to −0.8	−0.5 to −0.8
SM_3	CSI CS615	−1.2 to −1.5	−1.2 to −1.5	−1.2 to −1.5	−1.2 to −1.5
Observation periods					
1997	29 June to 12 July	3 July to 12 July	30 June to 12 July	2 July to 12 July	
1998	24 March to 20 June	25 March to 20 June	27 March to 20 June	28 March to 20 June	

[a] R_{net}: net radiation, K_d: downward shortwave radiation, K_u: reflected shortwave radiation, T_{ir}: infrared (surface) temperature, T_a: air temperature, RH: relative humidity, U: wind speed, WD: wind direction, RF: rainfall, G: soil heat conduction, T_{soil}: soil temperature, SM_1: volumetric soil moisture at level 1, SM_2: volumetric soil moisture at level 2, and SM_3: volumetric soil moisture at level 3.

[b] REBS: Radiation Energy Balance Systems, Seattle, WA, USA; Eppley Laboratories, Newport, RI, USA; Everest Interscience, Fullerton, CA, USA; Met-One, Grants Pass, OR, USA; CSI: Campbell Scientific, Logan, UT, USA.

SW–NE transect through the patch (Fig. 2). Observations at each site are described in Table 1. Sensors were sampled at a 10 s interval and statistics were recorded every 10 min with the exception of rainfall, which was recorded minutely.

Meteorological methods for estimating evaporation generally require a fetch of 100 m or more. In the case of edge effect studies, the heterogeneity which violates the assumptions of meteorological methods, is precisely the subject of the research. For this reason, we sought an alternative method which could be applied with equal reliability anywhere in a forest patch. We chose to estimate transpiration in sample trees by monitoring sap flow using the heat dissipation technique (Granier, 1985, 1987). Two Granier-type thermal dissipation probes (model TDP-30, Dynamax, Houston, TX, USA) were installed in each of 18 trees, 9 each in near-edge and interior zones of the patch. Three of the most abundant tree species were selected, *V. montana* Lour. (Euphorbiaceae), *A. tonkinensis* A. DC. (Annonaceae), and *G. planchonii* Pierre (Guttiferae), with three individuals of each species monitored within each of the two sap flow observation zones. Because of the very high species diversity in the patch, we were unable to limit our selections to individuals with similar stem and crown diameter and crown exposure. Sapwood depth in each tree was estimated using dyeing and heat dissipation techniques. Crown dimensions and exposure were assessed visually in the field. Characteristics of sap flow trees are given in Table 2.

We surveyed the locations, species, and diameter at breast height (DBH) of 328 trees (all trees with DBH >5 cm) within and around the sap flow monitoring zones, and measured light extinction using a ceptometer (Model CEP, Decagon, Pullman, WA, USA), in order to estimate the spatial pattern of leaf area index (LAI) within and between the sap flow monitoring zones (Table 3).

Observations were conducted during two intensive field experiments during June–July 1997 and March–June 1998. Results presented in this report will focus on the 1998 observation period. For the 1998 experiment, meteorological measurements were made continuously between 26 March and 20 June 1998; sap flow measurements were made during 1 April to 18 June 1998. Only 6 of 18 sap flow probes

Table 2
Characteristics of sap flow trees during 1998 experiment

	Species	Crown area (m^2)	Stem radius (m)	Height (m)	Distance from edge (m)	Exposure
Edge zone						
E1	*V. montana*	17.49	0.0698	14	11.0	Good
E2	*V. montana*	17.74	0.1237	22	5.9	Good
E3	*V. montana*	18.39	0.0762	17	10.4	Poor[a]
E4	*A. tonkinensis*	18.33	0.0634	13	7.1	Poor[b]
E5	*A. tonkinensis*	15.49	0.0587	13	26.7	Good
E6	*A. tonkinensis*	16.37	0.0675	12	3.8	Poor[b]
E7	*G. planchonii*	12.83	0.0925	16	14.6	Poor[b]
E8	*G. planchonii*	27.07	0.1175	18	20.1	Good
E9	*G. planchonii*	32.12	0.1799	25	5.5	Poor[b]
Interior zone						
F1	*V. montana*	57.52	0.1475	18	75.5	Good
F2	*V. montana*	25.15	0.0748	14	52.6	Good
F3	*V. montana*	60.13	0.1543	18	59.6	Good
F4	*A. tonkinensis*	13.40	0.0800	12	79.4	Good
F5	*A. tonkinensis*	11.26	0.0735	15	99.8	Poor[b]
F6	*A. tonkinensis*	35.89	0.0822	15	105.8	Good
F7	*G. planchonii*	41.96	0.1575	23	62.5	Good
F8	*G. planchonii*	28.65	0.1373	20	71.8	Good
F9	*G. planchonii*	41.71	0.1269	19	77.0	Good

[a] Heavy vine infestation in crown.
[b] Interference with sunlight and air flow due to overhanging and/or intertwining branches of other trees.

Table 3
Summary of tree survey

	Edge zone	Interior zone	Total
Number of trees surveyed	161	147	308
Number of tree species	68	66	105
Total basal area (m^2)	4.211	5.408	9.619
Estimated total active xylem area[a], $\sum A_x$ (m^2)	2.078	2.682	4.760
Surveyed area, A_s (m^2)	1965	2550	4515
$\sum A_x / A_s$	0.001058	0.001050	0.001054
Leaf area index[b]	2.67	2.19	2.40
Abundant tree species (count)			
G. planchonii Pierre (Guttiferae)	9	15	24
Archidendron clypearia (Jack) Niels. (Leguminosae, Mimosoideae)	17	4	21
V. montana Lour. (Euphorbiaceae)	7	7	14
Heteropanax fragrans (Roxb.) Seem. (Araliaceae)	9	5	14
Ostodes paniculata Bl. (Euphorbiaceae)	0	12	12
Schefflera heptaphylla (L.) Frod. (Araliaceae)	5	8	13
A. tonkinensis A. DC. (Annonaceae)	7	3	10
Macaranga auriculata (Merr.) A.S. (Euphorbiaceae)	8	0	8

[a] $\sum A_x$ is the sum of active xylem area values estimated for each surveyed tree using Eq. (6).
[b] LAI estimated using under canopy photosynthetically-active radiation (PAR) measurements in each 10 m × 10 m within each zone. Although we do not have sufficient measurements to quantify the trend, leave area in the canopy increased during the study period in response to the onset of rainy conditions.

were maintained during 24 April to 5 June 1998, while investigators were away at another field site. During that period, one tree of each species was selected for monitoring (with one probe each) in the forest edge and forest interior zones. The data derived from this subset of three sensors in each zone are referred to herein as "select", and comprise a complete record from 2 April to 17 June 1998.

3. Analysis

3.1. Sap flow analysis

The Granier (1985, 1987) sap flow method is analogous to the hot-wire anemometer technique for measuring wind. Each probe consists of a pair of 1.2 mm (o.d.) stainless steel needles installed into the tree stem about 4 cm apart in a vertical line. A constant voltage is applied to a resistor in the upper (heated) needle. A copper-constantan thermocouple measures the temperature difference between the heated upper needle and unheated lower reference needle. The flow of sap cools the heated needle. Laboratory experiments have shown that a reliable relationship exists between the observed temperature difference and the sap flux per unit sapwood area, i.e. the velocity of sap flow:

$$V = 0.0119 \left(\frac{\Delta T_{\max} - \Delta T}{\Delta T} \right)^{1.231} \quad (1)$$

where V is average sap flow velocity along the length of the probe ($\mathrm{cm\,s^{-1}}$), ΔT the temperature difference observed between the heated and reference needles, and $\Delta T_{\max}$ the value of ΔT when sap flow is zero (generally taken as the peak nighttime value of ΔT).

Clearwater et al. (1999) confirmed the original Granier (1985) calibration in the stems of tropical tree species. However, they showed that this calibration applied only when the entire length of the probe was in contact with conducting xylem (sapwood). When the length of the heated probe exceeds the thickness of conducting xylem, the original calibration underestimates sap velocity. They proposed a correction for Eq. (1) in which the ΔT of the sapwood (ΔT_{sw}) is computed as:

$$\Delta T_{\mathrm{sw}} = \frac{\Delta T - (b \times \Delta T_{\max})}{a} \quad (2)$$

where a and b are the proportions of the probe in sapwood and inactive xylem ($b = 1 - a$), respectively (Clearwater et al., 1999). It can be readily seen that this correction becomes very important as sapwood depth decreases below probe length. For many of the sample trees in our field study, this was the case. Hence, we replaced ΔT in Eq. (1) with ΔT_{sw} calculated with Eq. (2).

Sap flux (volume per unit time) can be computed as:

$$\mathrm{SF} = V \times A_{\mathrm{x}} \quad (3)$$

where A_{x} is the cross-sectional area of active xylem (sap-conducting wood). Transpiration of an individual tree can be estimated as:

$$\mathrm{Tr} = \frac{\mathrm{SF}}{A_{\mathrm{c}}} \quad (4)$$

where A_{c} is the projected ground area of the tree crown. Sap flow measurements can be used to scale up to the stand level as:

$$\overline{\mathrm{Tr}} = \frac{\bar{V} \times \sum A_{\mathrm{x}}}{A_{\mathrm{s}}} \quad (5)$$

where $\overline{\mathrm{Tr}}$ is the mean stand level transpiration, $\bar{V}$ the average sap velocity of monitored trees, $\sum A_{\mathrm{x}}$ the total cross-sectional area of active xylem for all trees in the stand, and A_{s} the stand ground area. By measuring A_{x} in a representative sample, a statistical relationship can be developed between A_{x} and tree stem radius (see below). The ratio $\sum A_{\mathrm{x}}/A_{\mathrm{s}}$ can be estimated by applying that relationship to the list of stem radius values obtained from a field survey of the stand (Table 3).

3.2. Sapwood depth

In light of Eq. (2), determination of the sapwood depth in monitored trees is an essential prerequisite for accurate interpretation of sap flow data. In many studies, sapwood is identified by visual inspection the wood coloration pattern of a severed stem or a core extracted with an increment borer. Some researchers inject dye into the transpiring stem before coring or severing the stem above the injection site. We found natural wood coloration of cores to give very little evidence of the active xylem region in our studied trees. During 1997 and 1998 field experiments, we injected dye into monitored trees. Subsequent cores gave unambiguous results in only a few trees. Dye was very

sparse or absent in the cores of 7 out of 18 trees, including all 6 *Garcinia* individuals. Uncertainty in sapwood depth estimates is an important issue in the use of Granier-type probes (James et al., 2002). In an effort to address this problem, a thermal dissipation probe was developed, in which a 1 cm-long heater and thermocouple were thermally isolated at the tips of plastic tubing (James et al., 2002). With this design, the sensor response is limited to sap flow in a narrow zone at the depth of the probe tips. By sequentially moving the probe to various depths, the resulting ΔT profile can be used to differentiate active and inactive xylem regions, and hence determine sapwood depth. Botany Department, University of Hawaii (Honolulu, USA) and Hawaii Agricultural Research Center (Honolulu, USA) staff built six 10 cm probes for our use at the Ban Tat study site. During November 1999, 16 of the original 18 sap flow trees (one tree had been felled, apparently to obtain fruits, the other had died) were resurveyed using these adjustable-depth probes. Combining the dye injection-coring results from June 1998 with the thermal dissipation probe results obtained in November 1999, a good relationship ($r^2 = 0.82$) was developed between sapwood depth and stem radius (Fig. 3). Data from all three species were combined to obtain the linear equation:

$$\mathrm{XD} = 0.01325 + 0.29856 \times \mathrm{SR} \quad (6)$$

where XD is xylem depth (cm) and SR is stem radius (cm). In tropical forest in Panama, Meinzer et al. (2001) similarly found the sapwood depth–stem size relationship to be consistent throughout a stand, independent of species. Applying this relationship to each of the surveyed trees gives estimates of $\sum A_x/A_s$ for edge and interior zones (Table 3).

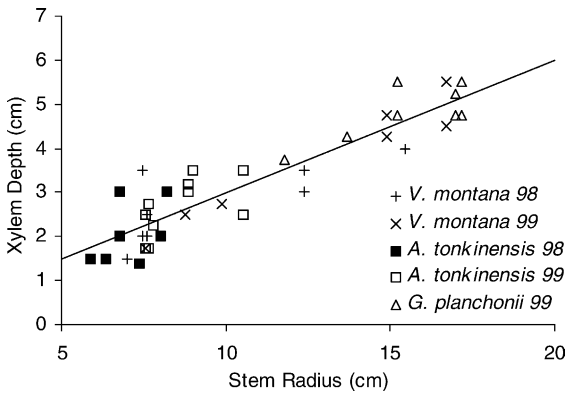

Fig. 3. Relationship between xylem depth and stem radius for 1998 sap flow trees. Points are based on dye injection-coring results from June 1998 and ΔT profile observations made in November 1999 using Burns–Holbrook-type probes.

3.3. Evaporation methods

Over homogeneous vegetated surfaces, a one-dimensional energy balance approach can be used to estimate total evaporation. The method can be expressed as (Monteith, 1973):

$$\lambda E = R_{\mathrm{net}} - G - H \quad (7)$$

where λ is the volumetric latent heat of vaporization ($\mathrm{J\,m^{-3}}$), E the evaporation ($\mathrm{m\,s^{-1}}$), R_{net} the net radiation ($\mathrm{W\,m^{-2}}$), G ($\mathrm{W\,m^{-2}}$) the soil heat conduction, and H ($\mathrm{W\,m^{-2}}$), sensible energy flux to the atmosphere, is estimated according to the resistance method:

$$H_{\mathrm{resistance}} = \frac{\rho C_{\mathrm{p}}(T_0 - T_{\mathrm{a}})}{r_{\mathrm{a}}} \quad (8)$$

where ρ is air density ($\mathrm{kg\,m^{-3}}$), C_{p} the specific heat of air at constant pressure ($\mathrm{J\,Kg^{-1}\,K^{-1}}$), T_0 the temperature at the virtual source/sink height for sensible heat exchange (K), T_{a} the air temperature (K), and r_{a} the aerodynamic resistance ($\mathrm{s\,m^{-1}}$). Measured infrared surface temperature may be substituted for T_0 (Hatfield et al., 1984; Choudhury et al., 1986). Aerodynamic resistance can be estimated as a function of wind speed, atmospheric stability, and the aerodynamic characteristics of the canopy parameterized in terms of the zero plane displacement height (d), the roughness length for momentum (z_0), and the roughness length for sensible heat transfer (z_{0h}). Stability corrections for estimating aerodynamic resistance appropriate for use with infrared surface temperature measurements were recommended by Choudhury et al. (1986).

Eq. (8) describes sensible heat transport to a level well above the canopy. At the two measurement sites within the forest patch (302 and 303), sensors were above the canopy of the trees in the immediate area, but below the level of some of the taller trees. Hence, an alternative method of estimating H may be more appropriate at these two sites. Brenner and Jarvis (1995)

describe a sensible heat flux method based on estimated leaf boundary-layer conductance (g_a^h):

$$H_{\text{boundary-layer}} = \rho C_p (T_0 - T_a) g_a^h \quad (9)$$

where g_a^h can be derived as a function of wind speed and characteristic leaf dimension. For a given leaf geometry, g_a^h can be approximated using:

$$g_a^h = au^b \quad (10)$$

where a and b are empirical coefficients (Brenner and Jarvis, 1995). The value of a ranges from 0.023 for a laminar boundary-layer to 0.034 for a turbulent boundary-layer. The exponent b, ranges from 0.5 (laminar) to 0.8 (turbulent). For low wind speeds ($<2.7\,\text{ms}^{-1}$), flow is approximately laminar.

Net radiation and soil heat flux were measured at only two of four stations (301 and 303). Net radiation was estimated at stations 302 and 303 as:

$$R_n = K_d - K_u + \varepsilon A - \varepsilon\sigma T_0^4 \quad (11)$$

where K_d is the downward shortwave radiation, K_u the reflected shortwave radiation (measured at station 303), ε the emissivity of the surface, A the downward longwave radiation from the atmosphere, and σ = 5.67E−8 (Stefan–Botlzmann constant). We assumed that solar radiation did not vary spatially over the study area; therefore, K_d measured at 301 was used to estimate R_{net} at 302 and 304. The vegetated surfaces at 302 and 304 were assumed to have albedos similar to that of station 303, therefore, K_u measured at 303 was substituted for R_{net} estimates at 302 and 304. Infrared measurements of surface temperature at 302 and 304 were used for T_0 at the respective sites. We assumed that downward longwave radiation did not vary over the study area, allowing us to estimate εA for both 302 and 304 as:

$$\varepsilon A = R_{net} - K_d + K_u + \varepsilon\sigma T_0^4 \quad (12)$$

where R_{net}, K_d, K_u, and T_0 were all measured at station 301.

Soil heat conduction (G) was estimated at each of two sites (301 and 303) on the basis of measurements of two flux plates inserted at a depth of 8 cm and a four-sensor averaging soil temperature probe with probes inserted at depths of 2 and 6 cm. G was estimated as the average of the two flux plate measurements plus the change in sensible heat in the 0–8 cm soil layer; soil specific heat was estimated as a function of the measured soil moisture in the upper 30 cm. At stations 302 and 304, where G was not measured, estimates from station 303 were substituted.

Land cover heterogeneity at the study site may reduce the reliability of the energy balance approach (Eq. (7)). For our clearing (station 301) and forest interior (station 302) sites, fetch over the respective surface is adequate under typical daytime conditions. The forest edge (302) and secondary vegetation edge (304) sites are often affected by the nearby land cover discontinuity, violating the assumptions of this method. However, the approach has been shown to be more reliable than other methods for locations affected by upwind heteorogeniety. Blad and Rosenberg (1976), for example, using the resistance formulation for H, found the method to perform well under both non-advective and strongly advective conditions. Brenner and Jarvis (1995) were able to apply the boundary-layer conductance approach to estimate H for locations at different distances downwind of a windbreak. However, they found that the values of the coefficients in Eq. (10) varied significantly with distance from the windbreak.

4. Observations and discussion

4.1. Meteorological conditions

With few exceptions, the conditions at the study site during the 1998 measurement period were characterized by high humidity and light winds (Fig. 4). Dew usually occurred during the early morning hours and forest vegetation often remained wet until 0930 local time. Solar and net radiation were frequently reduced by overcast. For these reasons, we would expect transpiration rates to be relatively low. The observation period straddles the onset of the summer monsoon and therefore includes the transition in moisture conditions associated with the increase in rainfall during mid-May 1998. Soil moisture content (Fig. 4f) clearly reflects the abrupt monsoonal transition. Although regional winds were dominantly southwesterly during most of the observation period, surface wind direction was strongly influenced by the mechanical and thermal effects of local topography and land cover. As a result, daytime winds were generally either

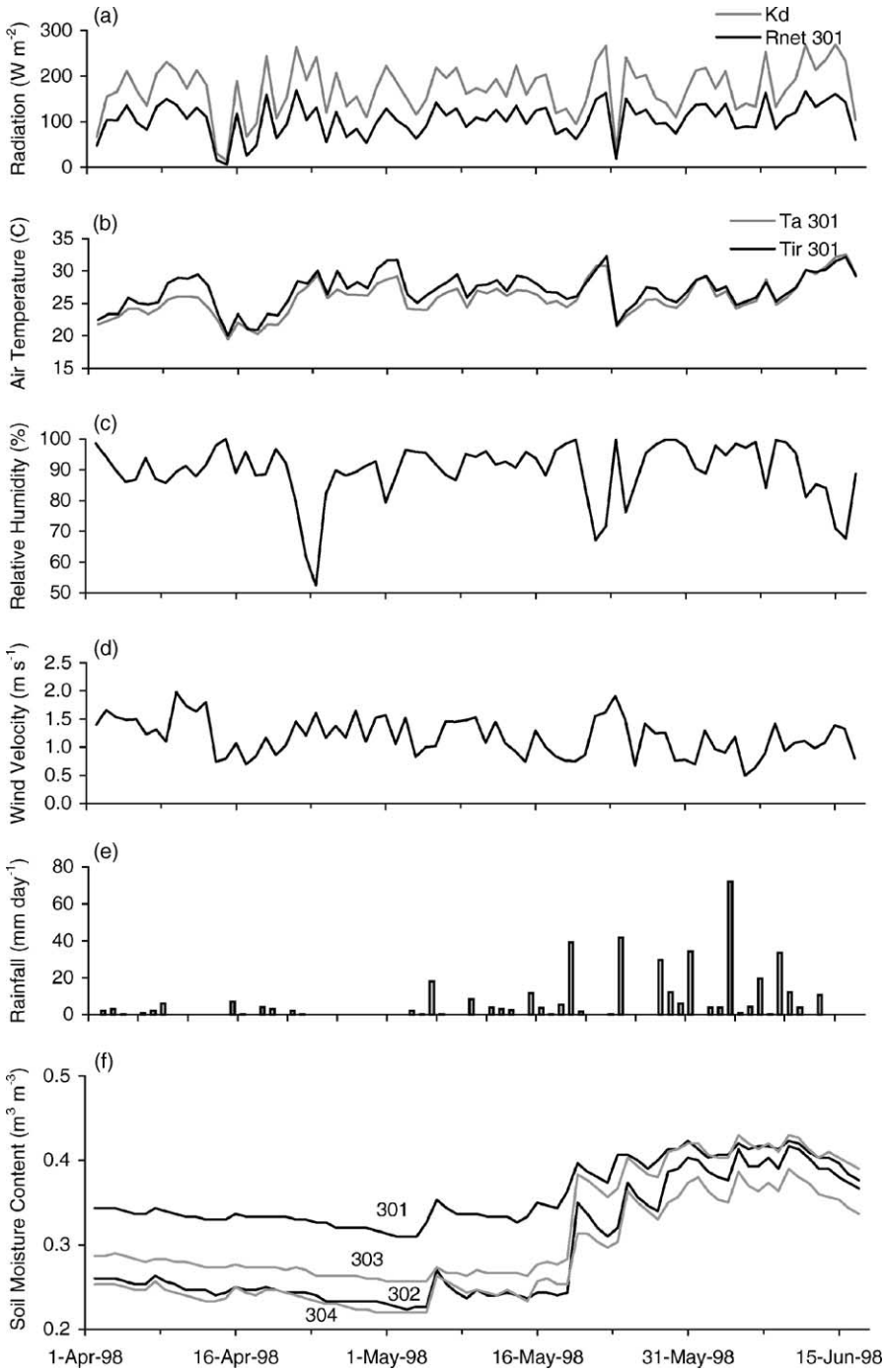

Fig. 4. Meteorological conditions during the 1998 observation period: (a) daily mean solar and net radiation, (b) daily mean air and surface temperature, (c) daily mean relative humidity, (d) daily mean wind velocity, (e) daily total rainfall, and (f) daily mean volumetric soil moisture content.

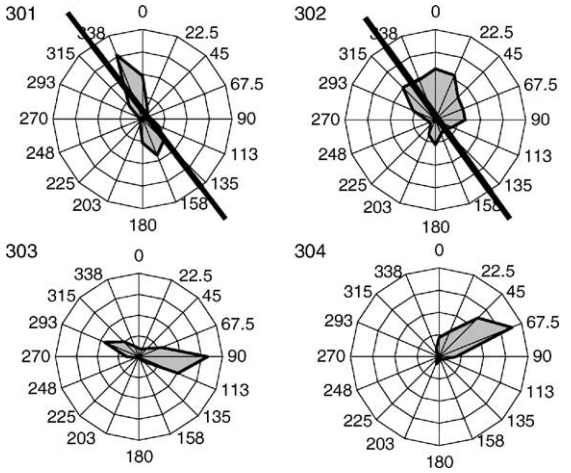

Fig. 5. Wind roses for the four meteorological stations within and near the forest patch study area, based on daytime periods during the 1998 observation period only. Lines show the approximate orientation of the forest boundary at the southwestern edge of the patch.

northwesterly or northeasterly and differed somewhat from site to site (Fig. 5).

The effects of proximity to the forest edge can be seen in the gradients in mid-day air temperature, surface temperature, humidity, wind speed, and soil moisture content (Fig. 6). Here we focus on the three stations located from the swidden field (301) to the forest interior (303). Data indicate a weak trend in daytime air temperature, with temperature declining toward the interior of the patch. The mid-day surface temperature of the swidden field site was dramatically higher than those of the forest edge or interior, as expected. Note that for the forest edge site, surface temperature was less than air temperature, indicating downward sensible heat flux (positive heat advection), and was markedly lower than the surface temperatures of the swidden field or the canopy temperature of the forest interior. The depressed mid-day surface temperature indicates high latent heat flux at the forest edge. Mean relative humidity (RH) increased toward the forest interior. The low RH over the swidden field results from higher temperatures and reduced

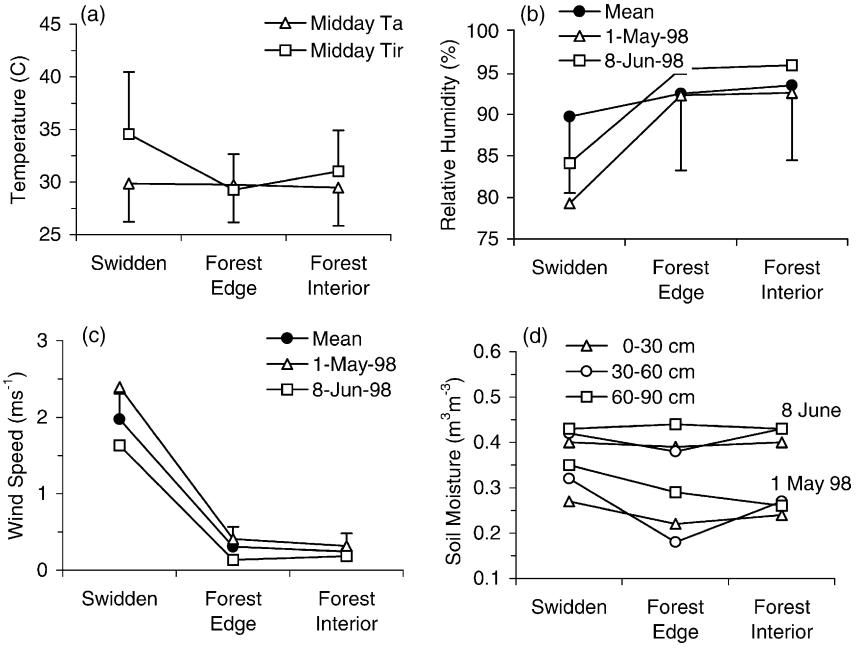

Fig. 6. Horizontal gradients of (a) mid-day (12:00–14:00) air temperature (T_a) and infrared canopy (surface) temperature (T_{ir}), (b) relative humidity, (c) wind speed, and (d) soil moisture in three depth layers near the forest edge. Shown are means for the 1998 study period, except where dates are given, in which case 1 day mean values are given. Error bars for the study period means show the standard deviation of daily values.

evapotranspiration over the sparsely vegetated surface. For comparison, mean wind speed at each site is adjusted to a common reference height 3 m above the respective zero plane displacement height. The higher wind speed seen over the smoother surface of the swidden field is reduced dramatically over the forest edge and interior sites.

The soil moisture profiles for 1 May (Fig. 6d) suggests that dry season soil extraction by roots, especially in the 30–60 cm layer (and hence transpiration of plants with roots in that layer), had been greater at the forest edge site than at the swidden field or forest interior sites (assuming similar soil water retention properties and similar soil moisture content at the start of the dry season). This pattern can also be seen in the daily time series of 0–90 cm soil moisture (Fig. 4f). This finding is similar to that of Kapos (1989) at an Amazonian site. In the 60–90 cm layer, however, dry season soil water extraction was apparently greatest at the interior site. By the time of the 8 June profile, despite the persistent rains that had been recharging soil moisture for several weeks, the lowest 30–60 cm soil moisture was again found at the forest edge site. 1 May soil moisture at all three levels was highest at the swidden field site. This reflects depressed dry season evaporation of bare soil sites. These observations are generally consistent with the Veen et al. (1996) depiction of the forest edge as a high-flux environment, i.e. a zone which actively absorbs thermal energy advected from surrounding cleared areas, damps wind speed, and transpires at a relatively high rate.

4.2. Sap flow

Analysis of the 1997 sap flow observations was limited to five of the six *V. montana* individuals used in 1998 (E1, E2, F1, F2, and F3). Transpiration in the sample trees was estimated using Eq. (4). Mean transpiration during 4–11 July 1997 is shown in Fig. 7 as a function of distance from the edge of the patch. These results suggested that transpiration was enhanced by proximity to the swidden field. However, the significance level of the slope was not sufficient to draw firm conclusions regarding edge effect. The value of the 1997 measurements was limited by the small number of sample trees, the use of only one species, and the short duration of the measurements.

The 1998 observations were more comprehensive in the number of individuals, number of species, and the period of observation. For the 1998 period, statistics of sap velocity, computed with Eq. (1), and transpiration, based on Eq. (4), are summarized for each sample tree in Table 4. Statistics are shown for the dry period (through 19 May), wet period (beginning 20 May), and the whole period (1 April to 17 June).

Significant differences in sap velocity were found among species and among individual trees. In general, velocities were greatest for *V. montana*, and least for *G. planchonii*. There were no clear differences in sap velocity between edge and forest interior trees. In general, mean sap velocity decreases with increasing stem size. Meinzer et al. (2001) found a strong negative exponential relationship ($r^2 = 0.88$) between sap velocity and stem size within a diverse stand of tropical trees

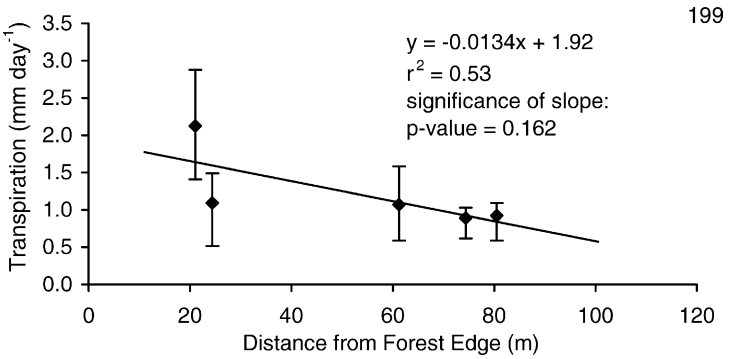

Fig. 7. Sap flow-derived transipiration in five *V. montana* individuals as a function of distance from the edge of the patch; based on observations taken during 4–11 July 1997 within the forest patch study area.

Table 4
Summary of sap flux density and transpiration estimates for individual trees

Zone	Tree	Species	Sap velocity (cm per day) mean ± S.D.			Transpiration (mm per day) mean ± S.D.		
			Dry[a]	Wet[a]	Whole period	Dry[a]	Wet[b]	Whole period
Edge	E1[c]	*V. montana*	14.8 ± 4.7	19.7 ± 7.3	16.7 ± 6.3	1.49 ± 0.48	1.99 ± 0.74	1.68 ± 0.63
	E2	*V. montana*	6.0 ± 2.1	14.2 ± 4.1	8.9 ± 4.9	1.93 ± 0.68	4.55 ± 1.32	2.86 ± 1.58
	E3	*V. montana*	4.8 ± 1.9	13.4 ± 4.8	7.8 ± 5.3	0.56 ± 0.23	1.54 ± 0.57	0.91 ± 0.61
	E4	*A. tonkinensis*	4.9 ± 1.9	10.7 ± 3.2	7.0 ± 3.7	0.40 ± 0.16	0.87 ± 0.26	0.57 ± 0.30
	E5	*A. tonkinensis*	10.0 ± 3.3	21.6 ± 5.9	14.1 ± 7.1	0.82 ± 0.27	1.77 ± 0.48	1.15 ± 0.58
	E6[c]	*A. tonkinensis*	6.6 ± 2.6	12.3 ± 5.3	8.7 ± 4.8	0.68 ± 0.27	1.28 ± 0.55	0.90 ± 0.49
	E7	*G. planchonii*	3.2 ± 1.3	5.7 ± 2.3	4.0 ± 2.1	0.77 ± 0.31	1.37 ± 0.56	0.98 ± 0.50
	E8[c]	*G. planchonii*	4.1 ± 1.6	4.6 ± 2.8	4.3 ± 2.1	0.76 ± 0.29	0.86 ± 0.53	0.80 ± 0.40
	E9	*G. planchonii*	1.5 ± 0.6	2.9 ± 1.5	2.0 ± 1.2	0.56 ± 0.21	1.08 ± 0.57	0.74 ± 0.45
Forest	F1	*V. montana*	6.2 ± 2.4	15.2 ± 3.7	9.5 ± 5.2	0.88 ± 0.34	2.15 ± 0.52	1.34 ± 0.74
	F2[c]	*V. montana*	15.1 ± 5.2	25.2 ± 9.4	18.9 ± 8.6	1.25 ± 0.43	1.92 ± 0.80	1.50 ± 0.67
	F3	*V. montana*	8.3 ± 2.7	13.9 ± 3.7	10.3 ± 4.1	1.22 ± 0.40	2.05 ± 0.55	1.52 ± 0.61
	F4	*A. tonkinensis*	6.5 ± 2.2	11.6 ± 3.2	8.3 ± 3.6	1.15 ± 0.39	2.07 ± 0.58	1.48 ± 0.64
	F5	*A. tonkinensis*	2.7 ± 0.8	5.0 ± 1.4	3.5 ± 1.5	0.49 ± 0.15	0.90 ± 0.25	0.64 ± 0.27
	F6[c]	*A. tonkinensis*	3.9 ± 1.1	7.6 ± 3.1	5.3 ± 2.7	0.27 ± 0.08	0.52 ± 0.22	0.36 ± 0.19
	F7	*G. planchonii*	4.1 ± 1.6	8.2 ± 2.7	5.6 ± 2.9	0.89 ± 0.35	1.78 ± 0.59	1.21 ± 0.62
	F8[c]	*G. planchonii*	2.6 ± 0.8	3.8 ± 1.5	3.0 ± 1.3	0.62 ± 0.20	0.93 ± 0.35	0.74 ± 0.31
	F9	*G. planchonii*	2.0 ± 0.8	3.4 ± 1.3	2.5 ± 1.2	0.29 ± 0.11	0.48 ± 0.18	0.36 ± 0.17

[a] 1 April to 19 May.
[b] 20 May to 17 June.
[c] Only the trees indicated with asterisks were monitored during the period 24 April to 5 June. Summary statistics are given for the three "select" trees over the full observation.

in Panama. We also found a significant ($P = 0.05$) negative exponential relationship for our sample trees, but it was rather weak ($r^2 = 0.23$). Sap velocity versus stem size for *A. tonkinensis* and *G. planchonii* fell reasonably close to the relationship found by Meinzer et al. (2001). Differences among species are even more apparent in terms of transpiration. *V. montana* transpired at about twice the rate of *A. tonkinensis*, and *G. planchonii*. Other sap flow-based studies have found contrasts in sap velocity and transpiration among different species (e.g. Granier et al., 1996; Schaeffer et al., 2000). Even for the same species, transpiration rates were quite variable among individual trees.

4.3. Total evaporation

We estimated total evaporation (λE) at each of the four meteorological stations using Eq. (7) with the resistance formulation for H (Eq. (8)). Aerodynamic parameters were estimated based on vegetation height and density, and, in the case of the swidden field site (301), the soil surface roughness. For the swidden field site (301), a crop was planted at about the same time as our observations began. Roughness of the soil surface, tree stumps, and cut vegetation was judged to be equivalent to 1.15 m-tall vegetation. At the end of the study, the crop had reached 2 m in height. The parameters z_0 and d for that site were assumed to increase linearly with time during the observation period; z_0 started at 0.13 m and increased at 0.0011 m per day; d started at 0.65 and increased at 0.0058 m per day. Mean vegetation height was estimated to be 16 m for the whole forest patch (though lower in the vicinity of the two stations 302 and 303, and 3.1 m at station 304. Constant values of z_0 and d were used for these three sites; $z_0 = 1.8$, 1.8, and 0.35 m, and $d = 8$, 7, and 2.45 m at 302, 303, and 304, respectively. At all sites, z_0 was set to $0.113h$, where h is the vegetation height. Here we used a higher value of z_0/h, conventionally set at 0.1, to account for effects of rough terrain and variable canopy height. The ratio z_0/z_{0h} was assumed to be 0.1. The value of d was shifted from a typical setting of $0.65h$ in an attempt to account for differences in vegetation density.

For sites 302 and 303, Eqs. (9) and (10) were used as an alternative method of estimating H. The coefficients in Eq. (10) were set at mid-range values, $a = 0.30$ and $b = 0.65$. To check the sensitivity of these estimates to changes in a and b, we made estimates of λE with parameters set for the extremes of laminar and turbulent boundary-layer conditions. We found the λE estimate at 302 to be insensitive to the method (using $H_{\text{resistance}}$ or $H_{\text{boundary-layer}}$) and to the selection of parameter values for Eq. (10). The mean $\lambda E/R_{\text{net}}$ ratio for station 302 was 0.970 using the resistance method, and 1.002, 0.998, and 0.993, for the boundary-layer method using coefficients set for laminar, mid-range, and turbulent conditions, respectively. At station 303, the estimate was more sensitive to the method used, with a mean $\lambda E/R_{\text{net}}$ ratio of 0.663 for the resistance method, and 0.825, 0.867, and 0.869 for the boundary-layer method using the three different sets of coefficient values. The higher λE values derived using $H_{\text{boundary-layer}}$ for the forest interior site are more conservative with respect to showing λE enhancement at the forest edge. The differences due to selection of Eq. (10) coefficients are not large. Therefore, we will present λE for stations 302 and 303 based on the boundary-layer approach with coefficients set at mid-range values. For the other two sites, we present λE derived using the resistance method. If we had elected to use the resistance method for all four sites, qualitative results (e.g. relative ordering of λE among the four sites) would not have been affected.

The time series of daily daytime (0:800–18:00 local time) λE and the fraction of net radiation used for evaporation ($\lambda E/R_{\text{net}}$) at the four stations are shown in Fig. 8. Means are derived from measurements and calculations at a 10 min interval, then averaged for the daytime period. Periods with rainfall are included. λE

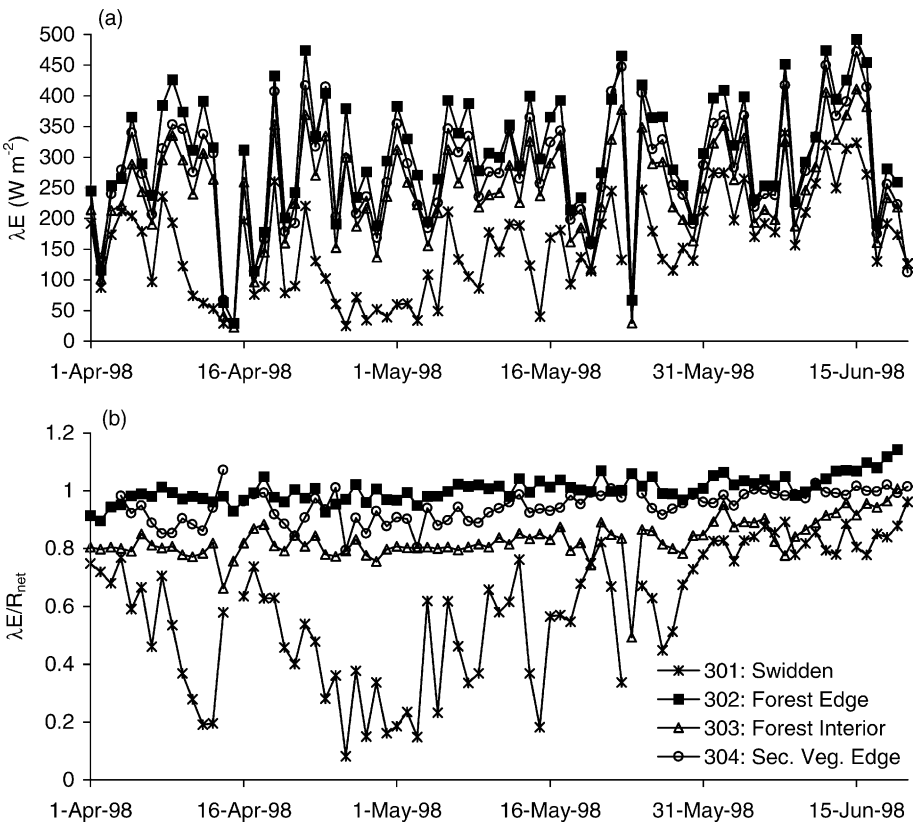

Fig. 8. Time series of total evaporation estimated using an energy balance approach for four stations in the forest patch study area: (a) daily evaporation (given in latent energy units (W m^{-2})) and (b) the ratio of latent heat flux to net radiation.

at all four stations increased during the study period, as would be expected in response to improving soil moisture availability and increasing LAI. Comparing the first and last 5-day periods in the study, λE increased 18, 17, 20, and 10% at the four sites 301–304, respectively. At 301, λE was highly responsive to day-to-day variations in soil moisture. The maximum daily λE rate during wet conditions at the end of the study was nearly four times as great as that of the minimum daily rate during the driest period in late April. Throughout the study period, the magnitude of λE varied by site, with $\lambda E_{302} > \lambda E_{304} > \lambda E_{303} \gg \lambda E_{301}$. This ordering can be seen more clearly in terms of $\lambda E/R_{net}$ (Fig. 8b).

4.4. Sap flow versus total evaporation

The energy equivalent of daily sap flow-based transpiration (24 h means) for edge and interior zones (Eq. (5)) are compared with estimated daily λE (24 h means) in Fig. 9. Only transpiration measurements based on the full array of sensors are used here; hence, the period 25 April to 5 June is excluded. It is apparent from the scattergrams (Fig. 9), that relationship between transpiration and λE differed for the early (dry) and late (wet) periods. The proportion of λE accounted for by transpiration in sampled canopy trees increased from 0.39 to 0.60 at the edge and from 0.43 to 0.68 in the interior. The relative contribution of the canopy transpiration is lower than generally found in other studies (e.g. Willschleger et al., 2001). The increases in transpiration as a proportion of λE correspond to increases in transpiration in both zones from <40% to about 60% of net radiation over the course of the observation period. In general, the difference between transpiration and total evaporation may be explained by (1) evaporation of intercepted rainfall, fog, and dew, (2) understory evapotranspiration, (3) soil evaporation, (4) errors in sap flow estimates due to uncertainties in sap flow probe measurements, xylem depth, and basal area, (5) errors in total evaporation estimates due to uncertainties in meteorological observations and parameter values, and violation of model fetch requirements. During wet conditions, we would expect interception evaporation and soil evaporation to become more important components of λE, and transpiration, therefore to decrease as a fraction of λE. For example, in a high-latitude forest, Kelliher et al. (1998) found that the relative contribution of the understory to total evaporation reached 54%, the highest level observed during their study, on the day immediately following a significant rainfall event. Our findings here are contrary to those expectations. We believe this result is due to the obvious increase in LAI of the sampled canopy trees observed (but not measured) during the study period. Under this scenario,

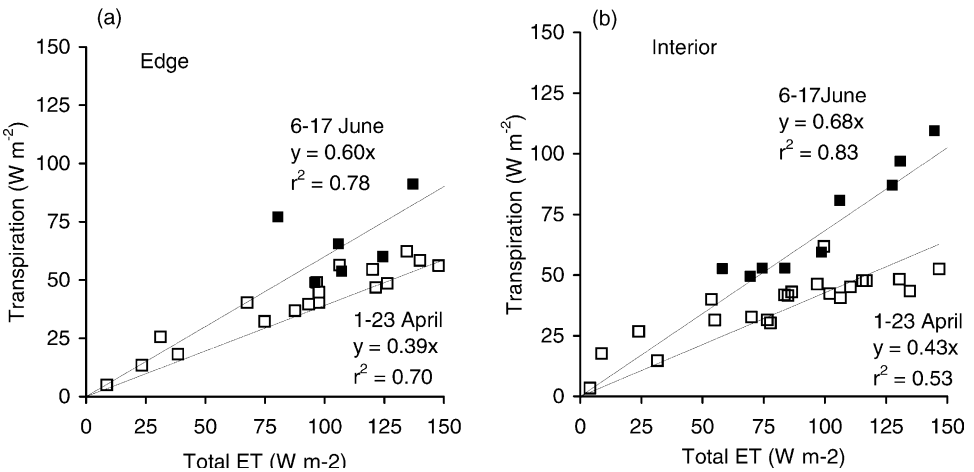

Fig. 9. Scattergrams of daily evaporation estimated using an energy balance approach and transpiration derived from sap flow measurements for forest edge and forest interior. Regressions are shown for dry (1–23 April) and wet (6–17 June) periods. Data omitted for period with reduced number of sensors (24 April to 5 June).

the understory, whose LAI did not increase as noticeably, would contribute proportionately less to λE as the canopy LAI increased. Because our LAI measurements were not taken systematically through time, we cannot give quantitative estimates of this effect.

4.5. Edge effect

4.5.1. Total evaporation

Comparing total evaporation among the four meteorological stations (Fig. 8) strongly suggests that surrounding cleared lands influence the spatial pattern of evaporation within the patch. This is most clearly seen in Fig. 8b, where site differences in R_{net} are controlled. Daily $\lambda E/R_{net}$ at the four sites are all statistically different from each other ($P < 0.0001$, paired comparison, *t*-test). Note that the two edge sites, stations 302 (over forest just inside the SW edge of the patch) and 304 (over secondary vegetation just outside the NE edge) consistently had the highest $\lambda E/R_{net}$ values. Evaporation at the forest interior station was intermediate between the rates of the swidden and edge sites. Toward the end (wetter) part of the observation period, λE of the forest interior site approached that of the two edge stations, suggesting that edge effect is greater under dry canopy conditions. In fact, the apparent enhancement of λE at the edge (relative to the interior) is greatest when λE in the adjacent clearing is depressed by dry soil conditions.

These findings are consistent with differences in soil moisture at the four sites (Fig. 4f). As mentioned, lower soil moisture at the two edge stations suggests greater cumulative dry season λE. Also, note that the slope of soil moisture content versus time during rainless periods (Fig. 4f), an indication of the λE rate, is greatest at the two edge sites.

4.5.2. Transpiration versus meteorological conditions

Daily edge and forest interior stand transpiration are well-correlated with daytime (0:800–18:00) atmospheric forcing variables measured in the clearing; solar radiation: $r = 0.739$ (edge) and 0.682 (interior); net radiation: $r = 0.743$ and 0.691; air temperature: $r = 0.721$ and 0.734; and relative humidity: $r = -0.523$ and -0.477. Transpiration in both stands is more highly correlated with R_{net}, T_a, and RH measured in the clearing than with corresponding measurements within the stands. These results suggest that transpiration in the forest patch is enhanced during relatively clear, sunny periods when the clearing is dry and hot, i.e. periods when conditions are conducive to high positive heat advection.

4.5.3. Comparison of zones

Transpiration estimates were scaled up from the individual tree level to stand level for the edge and forest interior zones using Eq. (5). A comparison of the two transpiration time series (not shown) reveals that the mean transpiration of the edge zone was consistently higher than that of the interior zone. The difference between the zones was greatest on days with relatively high rates of transpiration. To test the significance of the difference, we compare mean transpiration rates estimated from individual trees (Eq. (4)) in each zone (Table 5). Comparisons are made of zonal means based on all trees and for well-exposed trees (Table 2) only, and for the whole study period, dry period only, and

Table 5
Mean of individual tree transpiration means for edge and interior zones

Sample	Mean transpiration (mm per day) ± CV[a] edge (%)	*n*	Interior (%)	*n*	Difference (%)	*P*-value[b]
Whole	1.18 ± 59.9	9	1.02 ± 48.2	9	15.7	0.585
Whole: well-exposed	1.64 ± 51.3	4	1.06 ± 46.4	8	55.5	0.267
Dry	0.89 ± 56.3	9	0.78 ± 49.1	9	12.9	0.637
Dry: well-exposed	1.21 ± 43.9	4	0.78 ± 47.6	8	52.4	0.204
Wet	1.71 ± 66.7	9	1.42 ± 49.2	9	19.5	0.543
Wet: well-exposed	2.46 ± 59.3	4	1.56 ± 47.1	8	54.0	0.310

Values are given for the whole study period, the dry period (prior to 20 May), and the wet period (after 20 May).
[a] CV: coefficient of variation of individual tree means in each sample.
[b] Results of two sample *t*-test, assuming unequal variances.

wet period only. In all cases, mean values for the edge zone are higher than for the interior. However, due to the small sample size (number of trees) and the high variability among individual trees, none of the differences are statistically significant.

Lumping the transpiration measurements into two groups gives only a coarse picture of the spatial variability of transpiration within the patch. Below we evaluate one- and two-dimensional spatial patterns, looking for evidence of transpiration edge effect.

4.5.4. Spatial trend in transpiration

Variation in transpiration among individuals may be attributed to differences in (1) species, (2) location relative to the forest edge, (3) exposure due to vertical and horizontal position of crown relative to neighboring tree crowns (influenced in some cases by topography), (4) the amount of vine infestation, and (5) leaf area index. Evidence that differences in transpiration are related to proximity to the forest edge (item 2 above) may be obscured by the other factors listed above. Examining mean transpiration rates of individual trees as a function of location, indicates a statistically insignificant negative trend in transpiration with distance from the edge (Fig. 10, middle trend line). However, by selecting only well-exposed trees (Table 2) we obtain a better result. Well-exposed trees have higher mean transpiration rates than poorly-exposed trees, and a statistically significant trend with distance from the edge of -0.0135 mm per day m^{-1} (Fig. 10). The trend for poorly-exposed trees is not significant. It should be noted that the trend for well-exposed trees is strongly dependent on the high mean transpiration rate found for a single tree, E2. If we remove E2 from the sample of well-exposed trees, the trend is reduced in half, and the *P*-value increases from 0.02 to 0.13, i.e. it no longer meets our criterion for significance.

4.5.5. Mean 2D spatial patterns of transpiration

To examine the spatial patterns of transpiration within the patch, we analyzed the two-dimensional pattern using spatial mapping software (Surfer, Golden Software, Golden, CO, USA). Here we use all trees regardless of crown exposure, but attempt to remove differences among the three species by normalizing the data, dividing the transpiration rate of each tree by its respective species mean. Values were interpolated/extrapolated to a 1 m × 1 m grid using the Kriging option in Surfer. Default settings are used for all Kriging options except error nugget, which is set at 0.05. Fig. 11 shows the mean pattern of transpiration for the whole study period. The spatial pattern shown in Fig. 11 suggests transpiration enhancement near the edge. The spatial trend in transpiration extends through both the edge and interior zones, suggesting that transpiration edge effect extends at least 100 m

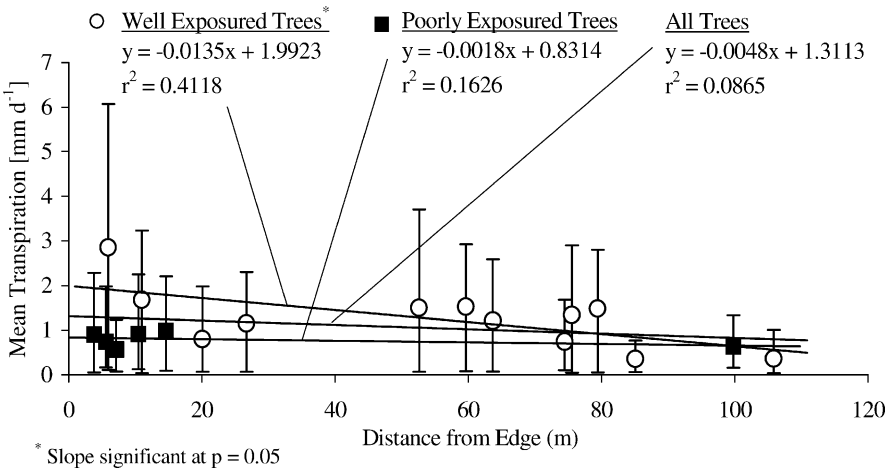

Fig. 10. Mean whole period transpiration of individual trees as a function of distance from the forest edge. Rates of well-exposed trees (those rated as having good or fair exposure to sunlight and wind) and poorly-exposed trees are shown as open circles and closed squares, respectively. Lines shown for well-exposed, poorly-exposed, and all trees, are based on regressions of mean transpiration versus distance from the forest edge.

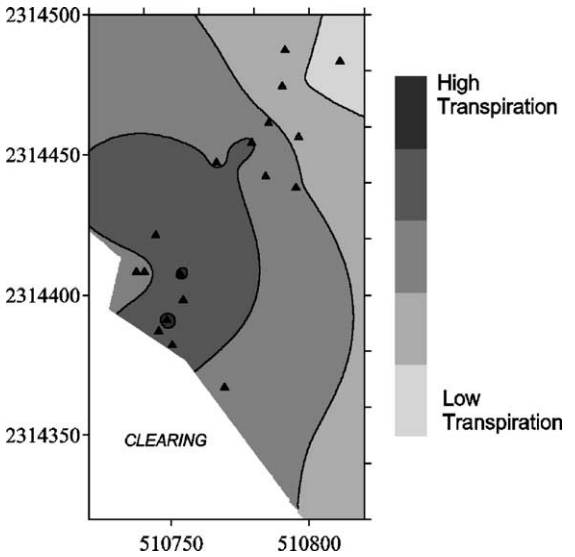

Fig. 11. Spatial patterns of normalized transpiration, based on means for the whole study period. Axis labels give UTM coordinates (m).

from the southwestern edge of the patch. The decreasing trends to the northwest and southeast of this peak are partly artifacts of extrapolation outside the observation areas.

The mean transpiration pattern (Fig. 11) suggests enhancement of transpiration along the southwestern edge of the patch despite the fact that wind in the adjacent clearing often was not oriented toward the patch. We expected to find edge effect chiefly when warmer drier air from the adjacent clearing moved into the patch. At the swidden station (located 45 m from the forest edge), daytime wind direction indicated flow crossing the patch boundary moving into the patch during only 32% of the daytime observations. Wind direction at that station is strongly influenced by the local topography, tending to flow parallel to the axis of the small valley there. Villagers who assisted us in the field maintained a small hut just outside the forest edge. We often observed smoke from their cooking fire to move parallel to the patch boundary, with eddies diffusing the smoke into the patch. We suspect that the movement of air across the southwest patch boundary from the clearing into the patch was more frequent than was indicated by measured wind direction at the clearing site. To verify that the observed transpiration pattern was influenced by the adjacent clearing, we examined variations in the pattern as it responded to different weather conditions, including wind direction.

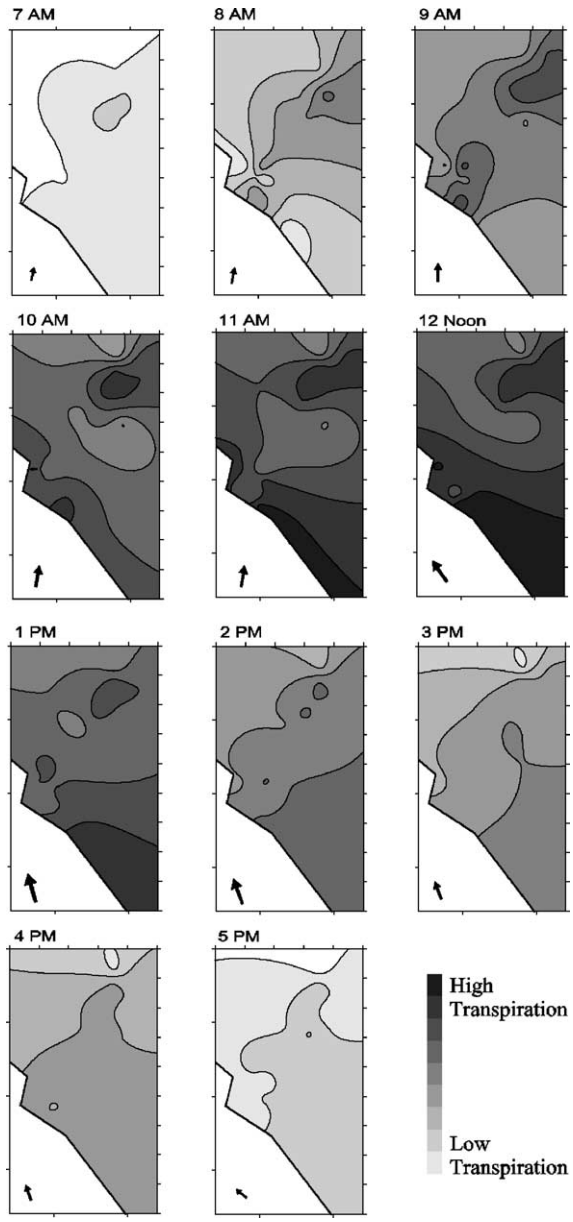

Fig. 12. Spatial patterns of normalized transpiration for hourly periods on 8 April 1998. Also shown is wind speed and direction in the clearing (size and orientation of arrow).

4.5.6. Changing spatial patterns of transpiration during 8 April

We analyzed the patterns of normalized transpiration for each hour during 8 April (Fig. 12) to determine whether response to short-term variation in wind direction could be observed in the spatial pattern of transpiration. Values were normalized using the mean dry-period transpiration for each tree. Arrows represent wind speed and direction in the clearing. Conditions on 8 April were partly cloudy with moderate humidity. Changes in transpiration during the day follow the diurnal cycles of radiation and relative humidity, with the highest values at mid-day. During the morning, winds were SSW to S in the clearing and E to ENE at the interior zone (not shown). As the day progressed, winds in the clearing shifted to SE, and at the interior were E to ESE. The spatial pattern during the morning was bimodal with peaks near the edge and at the NE corner of the interior zone. Enhancement at the edge peaked at mid-day. During the afternoon, the pattern changed as wind direction at the edge shifted, until by mid-afternoon, with wind then roughly parallel to the SW patch boundary, no edge enhancement was evident. The diurnal variation in the pattern near the edge confirms that edge effect is sensitive to edge orientation and wind direction. The morning and mid-day interior peak may be related to the easterly wind there. Although the patch extends several hundred meters east of this area, there is a gap in the canopy along the NE portion of the interior zone, and a steep downward slope in that direction. Trees at the extreme NE corner are exposed to easterly winds and transpiration appears to have been enhanced as a result. This is evidence that transpiration enhancement can occur not only at exposed forest edges, but also within the patch where topography or canopy structure exposes trees to energy advected from cleared land outside the patch.

5. Conclusions

Our field observations within and near a small forest patch in Ban Tat provide the following information regarding patch microclimate and transpiration:

1. The effects of proximity to the forest edge can be seen in the microclimatic gradients. Mid-day air temperature declined from the swidden field to the patch interior. Mid-day surface temperature was highest over the swidden field and lowest at the forest edge. Relative humidity increased into the patch. Reference height wind speed decreased sharply across the forest patch boundary.
2. Soil moisture content at the end of the dry season was lowest at the forest edge and secondary vegetation edge sites, suggesting greater cumulative dry season evapotranspiration there than at swidden and forest interior sites.
3. Considerable variability in transpiration was observed among trees, especially among different species.
4. As conditions became wetter, canopy transpiration as a fraction of total evaporation increased from 0.39 to 0.60 at the edge and from 0.43 to 0.68 in the interior. This unexpected finding may have been the result of increasing overstory LAI during the study period.
5. Daytime total evaporation was highest at the forest edge and secondary vegetation edge sites. The lowest daytime total evaporation was observed at the swidden site. The difference between evaporation at edge and the interior decreased as conditions became wetter.
6. Transpiration of both forest edge and interior zones is highly correlated with conditions in the adjacent swidden field. This implies that edge effect on transpiration is greatest when conditions are favorable for high positive heat advection from the clearing to the forest edge.
7. Mean transpiration rates of the edge and interior zones, based on averages of sap flow rates in all trees in each zone, were not significantly different.
8. Analyzing transpiration of each tree on the basis of distance from the edge, resulted in a statistically significant linear trend in average transpiration of -0.0135 mm per day m^{-1} for well-exposed trees. However, this trend is strongly dependent on the high transpiration rate of one individual tree.
9. The mean two-dimensional transpiration pattern suggests enhancement near the edge.
10. Hour-to-hour changes in the transpiration pattern were responsive to shifts in wind direction. However, it appears that, even in the patch interior, tree crowns exposed to advected energy because of topographic position or canopy structure, also experience enhanced transpiration.

The results obtained in this study show that the magnitude and spatial pattern of transpiration in small forest patches is strongly influenced by the conditions in surrounding clearings. However, transpiration enhancement can occur not only at forest edges, but also well within the patch for trees whose canopies are exposed to advection. The distance-to-edge dependency of transpiration for well-exposed trees, while suggesting that regional evapotranspiration (ET) is influenced by the degree of fragmentation, is not conclusively established by our observations. Although the magnitude and spatial extent of edge effects on transpiration remain uncertain, spatial differences in total evaporation and dry season soil moisture draw-down add to the evidence that ET of exposed forest edges is enhanced. If edges experience higher rates of ET, greater fragmentation would result in higher regional evaporative flux, i.e. other factors being equal, small patches would have higher ET rates than large patches. Hence, fragmentation of remaining forested areas would partly offset the reduction in regional evaporation due to deforestation.

The conclusions drawn from this study are limited by the relatively small number of trees (and species) sampled for transpiration, and the high variability of transpiration among sampled trees. Further, highly variable exposure due to the rough terrain and diverse canopy structure obscures the distance-to-edge dependency which may exist. It is likely that the type of replacement land cover, cultivation practices, fire frequency, and moisture status of the clearings, i.e. the degree of contrast of the surroundings or "matrix harshness" (Gascon et al., 2000), affect this process. We should also note that although we found greater differences in evaporative flux during the dry period, it is possible that under more prolonged or severe dry conditions, soil moisture storage at the forest edge would become depleted and leaf area would decline significantly leading to lower transpiration rates near the edge than in the interior.

Acknowledgements

This research was facilitated by numerous individuals associated with the East-West Center (EWC), Honolulu, the Center for Natural Resources and Environmental Studies (CRES), Vietnam National University, Hanoi, and Hanoi Agricultural University (HAU). We especially thank Jeff Fox and Steve Leisz (EWC), Le Trong Cuc (CRES), and Tran Duc Vien (HAU). We are greatly indebted to the kindness and skill of the Tat Hamlet residents, especially Lan, Lian, and Mai, who assisted our field work. This paper is based on work supported by the US National Science Foundation under Grant No. DEB-9613613.

References

Blad, B.L., Rosenberg, N.J., 1976. Evaluation of resistance and mass transport evapotranspiration models requiring canopy temperature data. Agron. J. 68, 764–769.

Brenner, A.J., Jarvis, P.G., 1995. A heated leaf replica technique for determination of leaf boundary layer conductance in the field. Agric. For. Meteorol. 72, 261–275.

Bruijnzeel, L.A., 1990. Hydrology of moist tropical forests and effects of conversion: a state of knowledge review. UNESCO, Paris and Vrije Universiteit, Amsterdam.

Bruijnzeel, L.A., 2001. Forest hydrology. In: J.C. Evans (Ed.), The Forests Handbook. Blackwell Scientific Publications, Oxford, UK (Chapter 12).

Chen, J., Franklin, J.F., Spies, T.A., 1993. Contrasting microclimates among clearcut, edge, and interior of old-growth Douglas-fir forest. Agric. For. Meteorol. 63, 219–237.

Choudhury, B.J., Reginato, R.J., Idso, S.B., 1986. An analysis of infrared temperature observations over wheat and calculation of latent heat flux. Agric. For. Meteorol. 37, 75–88.

Clearwater, M.J., Meinzer, F.C., Andrade, J.L., Goldstein, G., Holbrook, N.M., 1999. Potential errors in measurement of nonuniform sap flow using heat dissipation probes. Tree Physiol. 19, 681–687.

Famiglietti, J.S., Wood, E.F., 1994. Multiscale modeling of spatially variable water and energy balance processes. Water Resour. Res. 30, 3061–3078.

Famiglietti, J.S., Wood, E.F., 1995. Effects of spatial variability and scale on areally averaged evapotranspiration. Water Resour. Res. 31, 699–712.

Gascon, C., Williamson, G.B., da Fonseca, G.A.B., 2000. Receding forest edges and vanishing reserves. Science 288, 1356–1358.

Gash, J.H.C., 1986. A note on estimating the effect of a limited fetch on micrometeorological evaporation measurements. Boundary-Layer Meteorol. 35, 409–413.

Giambelluca, T.W., Hölscher, D., Bastos, T.X., Frazão, R.R., Nullet, M.A., Ziegler, A.D., 1997. Observations of albedo and radiation balance over post-forest land surfaces in eastern Amazon Basin. J. Climate 10, 919–928.

Giambelluca, T.W., Fox, J., Yarnasarn, S., Onibutr, P., Nullet, M.A., 1999. Dry-season radiation balance of land covers replacing forest in northern Thailand. Agric. For. Meteorol. 95, 53–65.

Granier, A., 1985. Une novuvelle méthode pour la mesure du flux de sève brute dans le tronc des arbres. Ann. Sci. For. 42, 193–200.

Granier, A., 1987. Evaluation of transpiration in a Douglas fir stand by means of sap flow measurements. Tree Physiol. 3, 309–320.

Granier, A., Huc, R., Barigah, S.T., 1996. Transpiration of natural rain forest and its dependence on climatic factors. Agric. For. Meteorol. 78, 19–29.

Hahmann, A.N., Dickinson, R.E., 1997. RCCM2_BATS model over tropical South America: applications to tropical deforestation. J. Climate 10, 1944–1964.

Hatfield, J.L., Reginato, R.J., Idso, S.B., 1984. Evaluation of canopy temperature–evapotranspiration models over various crops. Agric. For. Meteorol. 32, 41–53.

Henderson-Sellers, A., Gornitz, V., 1984. Possible climatic impacts of land cover transformations, with particular emphasis on tropical deforestation. Climatic Change 6, 231–257.

Henderson-Sellers, A., Dickinson, R.E., Durbridge, T.B., Kennedy, P.J., McGuffie, K., Pitman, A.J., 1993. Tropical deforestation: modeling local- to regional-scale climate change. J. Geophys. Res. 98, 7289–7315.

Hutjes, R.W.A., 1996. Transformation of near surface meteorology in a landscape with small scale forests and arable land. Ph.D. Dissertation, University of Groningen, The Netherlands.

James, S.A., Clearwater, M.J., Meinzer, F.C., Goldstein, G., 2002. Heat dissipation sensors of variable length for the measurement of sap flow in trees with deep sapwood. Tree Physiol. 22, 277–283.

Jipp, P.H., Nepstad, D.C., Cassel, D.K., Reis de Carvalho, C., 1998. Deep soil moisture storage and transpiration in forests and pastures of seasonally-dry Amazonia. Climatic Change 39, 395–412.

Kapos, V., 1989. Effects of isolation on the water status of forest patches in the Brazilian Amazon. J. Tropical Ecol. 5, 173–185.

Kapos, V., Wandelli, E., Camargo, J.L., Ganade, G., 1997. Edge-related changes in environment and plant responses due to forest fragmentation in central Amazonia. In: Laurance, W.F., Bierregaard, R.O. Jr. (Eds.), Tropical Forest Remnants: Ecology, Management, and Conservation of Fragmented Communities. University of Chicago Press, Chicago, USA, pp. 33–44.

Kelliher, F.M., Lloyd, J., Arneth, A., Byers, J.N., McSeveny, T.M., Milukova, I., Grigoriev, S., Panfyorov, M., Sogatchev, A., Varlargin, A., Ziegler, W., Bauer, G., Schulze, E.-D., 1998. Evaporation from a central Siberian pine forest. J. Hydrol. 205, 279–296.

Kienitz, G., Milly, P.C.D., Van Genuchten, M. Th., Rosbjerg, D., Shuttleworth, W.J. (Eds.), 1991. Hydrological Interactions Between Atmosphere, Soil and Vegetation. International Association of Hydrological Sciences Publication No. 204. IAHS Press, Wallingford, UK.

Klaassen, W., 1992. Average fluxes from heterogeneous vegetated regions. Boundary-Layer Meteorol. 58, 329–354.

Klaassen, W., Lankreijer, H.J.M., Veen, A.W.L., 1996. Rainfall interception near a forest edge. J. Hydrol. 185, 349–361.

Kruijt, B., Klaassen, W., Hutjes, R.W.A., Veen, A.W.L., 1991. Heat and momentum fluxes near a forest edge. In: Kienitz, G., et al. (Eds.), Hydrological Interactions Between Atmosphere, Soil and Vegetation. International Association of Hydrological Sciences Publication No. 204. IAHS Press, Wallingford, UK, pp. 107–116.

Laurance, W.F., Bierregaard, R.O. Jr., 1997. A crisis in the making. Preface to Laurance, W.F., Bierregaard, R.O. Jr. (Eds.), Tropical Forest Remnants: Ecology, Management, and Conservation of Fragmented Communities. University of Chicago Press, Chicago, USA.

Laurance, W.F., Ferreira, L.V., Rankin-de Merona, J.M., Laurance, S.G., 1998. Rain forest fragmentation and the dynamics of Amazonian tree communities. Ecology 79, 2032–2040.

Lean, J., Warrilow, D.A., 1989. Simulation of the regional climatic impact of Amazon deforestation. Nature 342, 411–413.

Liang, X., Lettenmaier, D.P., Wood, E.F., Burges, S.J., 1994. A simple hydrologically based model of land surface water and energy fluxes for general circulation models. J. Geophys. Res. 99, 14,415–14,428.

Matlack, G.R., 1993. Microenvironment variation within and among forest edge sites in the eastern United States. Biol. Conserv. 66, 185–194.

McGuffie, K., Henderson-Sellers, A., Zhang, H., Durbridge, T.B., Pitman, A.J., 1995. Global sensitivity to tropical deforestation. Global Planet. Change 10, 97–128.

Meinzer, F.C., Goldstein, G., Andrade, J.L., 2001. Regulation of water flux through tropical forest canopy trees: do universal rules apply? Tree Physiol. 21, 19–26.

Monteith, J.L., 1973. Principles of Environmental Physics. Elsevier, New York.

Murcia, C., 1995. Edge effects in fragmented forests: implications for conservation. TREE 10, 58–62.

Neal, C., Robson, A.J., Bhardwaj, C.L., Conway, T., Jeffery, H.A., Neal, M., Ryland, G.P., Smith, C.J., Walls, J., 1993. Relationships between precipitation, stemflow and throughfall for a lowland beech plantation, Black Wood, Hampshire, southern England: findings on interception at a forest edge and the effects of storm damage. J. Hydrol. 146, 221–233.

Nobre, C.A., Sellers, P.J., Shukla, J., 1991. Amazonian deforestation and regional climate change. J. Climate 4, 957–988.

Polcher, J., Laval, K., 1994. The impact of African and Amazonian deforestation on tropical climate. J. Hydrol. 155, 389–405.

Schaeffer, S.M., Williams, D.G., Goodrich, D.C., 2000. Transpiration of cottonwood/willow forest estimated from sap flux. Agric. For. Meteorol. 105, 257–270.

Shukla, J., Nobre, C., Sellers, P.J., 1990. Amazon deforestation and climatic change. Science 247, 1322–1325.

Stewart, J.B., Engman, E.T., Feddes, R.A., Kerr, Y. (Eds.), 1996. Scaling up in Hydrology Using Remote Sensing. Wiley, Chichester, UK.

Turton, S.M., Freiburger, H.J., 1997. Edge and aspect effects on the microclimate of a small tropical forest remnant on the Atherton Tableland, northeastern Australia. In: Laurance, W.F., Bierregaard, R.O. Jr. (Eds.), Tropical Forest Remnants: Ecology, Management, and Conservation of Fragmented Communities. University of Chicago Press, Chicago, USA, pp. 45–54.

Veen, A.W.L., Hutjes, R.W.A., Klaassen, W., Kruijt, B., Lankreijer, H.J.M., 1991. Evaporative conditions across a grass-forest boundary: a comment on the strategy for regionalizing evaporation. In Kienitz, G., et al. (Eds.), Hydrological Interactions Between Atmosphere, Soil and Vegetation.

International Association of Hydrological Sciences Publication No. 204. IAHS Press, Wallingford, UK.

Veen, A.W.L., Klaassen, W., Kruijt, B., Hutjes, R.W.A., 1996. Forest edges and the soil-vegetation-atmosphere interaction at the landscape scale: the state of affairs. Prog. Phys. Geogr. 20, 292–310.

Whitmore, T.C., 1997. Tropical forest disturbance, disappearance, and species loss. In: Laurance, W.F., Bierregaard, R.O. Jr. (Eds.), Tropical Forest Remnants: Ecology, Management, and Conservation of Fragmented Communities. University of Chicago Press, Chicago, USA.

Willschleger, S.D., Hanson, P.J., Todd, D.E., 2001. Transpiration from a multi-species deciduous forest as estimated by xylem sap flow techniques. For. Ecol. Manage. 143, 205–213.

Wright, I.R., Gash, J.H.C., Da Rocha, H.R., Shuttleworth, W.J., Nobre, C.A., Maitelli, G.T., Zamparoni, C.A.G.P., Carvalho, P.R.A., 1992. Dry season micrometeorology of central Amazonian ranchland. Q. J. R. Meteorol. Soc. 188, 1083–1099.

Xue, Y., Bastable, H.G., Dirmeyer, P.A., Seller, P.J., 1996. Sensitivity of simulated surface fluxes to changes in land surface parameterizations—a study using ABRACOS data. J. Appl. Meteorol. 35, 386–400.